ISSN 0965-5425, Computational Mathematics and Mathematical Physics, 2021, Vol. 61, No. 12, pp. 2118–2128. © Pleiades Publishing, Ltd., 2021.

MATHEMATICAL PHYSICS

Sound Radiation from Non-Uniformly Lined Duct with Partial Rigidity

B. Tiryakioglu[a]

[a] *Department of Applied Mathematics, Marmara University, Istanbul, 34722 Turkey*

e-mail: burhan.tiryakioglu@marmara.edu.tr

Received January 7, 2021; revised June 8, 2021; accepted September 9, 2021

Abstract—Radiation of sound waves by a semi-infinite circular cylindrical pipe with non-uniform lining is analyzed by using the Jones' method in conjunction with the mode matching technique. This mixed method of formulation gives rise to a scalar Wiener–Hopf equation. The inner surface of the duct is coated by acoustically absorbing different linings. In the present study, different linings with partial rigidity make the problem more interesting when it is compared with the uniform lining. The solution of the considered problem involves three infinite sets of coefficients satisfying three infinite systems of linear algebraic equations. Numerical solutions of these systems are obtained for various values of the parameters of the problem and their effects on the radiation phenomenon are shown graphically. The solution is compared graphically with a similar study existing in the literature. A perfect agreement is observed between the both results.

Keywords: Wiener–Hopf technique, mode matching method, Fourier transform, saddle point technique

DOI: 10.1134/S0965542521310031

1. INTRODUCTION

Analysis of sound wave propagation in waveguides with discontinuities has received wide attention due to its importance in acoustics. Up until now, numerous analytical and numerical studies have been derived [1–6]. One method of reducing noise is to introduce linings to absorb the noise as it travels along the pipe. The use of perforated screen in the semi infinite pipe is another method that has proved useful in reducing unwanted noise. The radiation of sound waves from a semi-infinite rigid pipe has been first considered by Levine and Schwinger [7] by using the Wiener–Hopf technique [8]. Wiener–Hopf technique has been used in acoustic problems extensively [9–12].

Rawlins proved that acoustically absorbing lining is an efficient method to reduce the irritated sound [13]. He analyzed the radiation of sound from an unflanged rigid cylindrical duct with an acoustically absorbing internal surface. Then, Demir and Buyukaksoy treated a similar problem with partial lining [14]. In their work, an alternative formulation based on the Mode Matching method in conjunction with the Fourier transforms technique was adopted. Recently, the acoustic radiation problem by a semi-infinite duct with perforated screen is analyzed rigorously by Tiryakioglu [15, 16]. In addition to all these studies, the absorbing lining has been investigated extensively with and without flow in the literature [17–20].

Keeping in view the aforementioned studies, the current study is designed to analyze the effects of different lining with partial rigidity. The geometry of the current problem under consideration is sketched in Fig. 1. The different linings with partial rigidity make the problem interesting when considering with uniform lining. Hence, here we incorporate the Wiener–Hopf and the mode matching method together to solve this theoretical model. By using the Fourier transform, the related boundary value problem is solved analytically with the help of sophisticated and suitable method known as Wiener–Hopf technique. The Wiener–Hopf technique is a mathematical method that could yield closed form analytic solutions for radiation/diffraction problems. The problem is then reduced directly into a Wiener–Hopf equation whose solution involves a set of infinitely many unknown expansion coefficients satisfying an infinite system of linear algebraic equations. The infinite systems of equations are solved by applying MATLAB programming. The linear system of equations converges rapidly, so we can truncate systems of equations in our calculation and estimate the solution. The introduction of different linings with partial rigidity, which is the main difference from previous studies, changes the continuity at the related point and the method of solu-

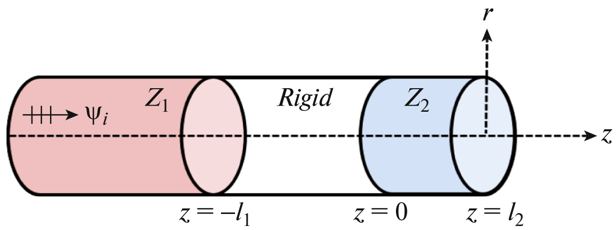

Fig. 1. Geometry of the problem.

tion requires a careful analysis in calculating the sound pressure level. This partial rigidity is very effective both mathematically and physically. One of our aims in this paper is to find out the influence of different linings and partial rigidity length on sound radiation.

Verification of the results of the present study is obtained numerically. The results are compared with the problem [14] where the solution is obtained for partial inner lining. It is found that for various values of the parameters, the agreement is excellent.

This article is organized as follows. The mathematical model is formulated in Section 2. The Wiener–Hopf equation and solution, which are obtained using a standard Wiener–Hopf procedure, are obtained with the help of Fourier transform technique in Section 3. Expansion coefficients and far field are presented in Sections 4 and 5, respectively. Some numerical illustrations are described in Section 6. To end with, final remarks are summarized in Section 7.

2. PROBLEM STATEMENT

Consider the radiation of sound waves by a semi-infinite non-uniform lined duct. Duct walls are assumed to be infinitely thin and they occupy the region $\{r = a, z \in (-\infty, l_2)\}$ (see Fig. 1). The outer surface of cylinder is assumed to be rigid while the inner surface of cylinder is assumed to be coated with two different absorbing lining. The liner impedance are characterized by Z_1 $(z \in (-\infty, -l_1))$ and Z_2 $(z \in (0, l_2))$, respectively. From the symmetry of the geometry of the problem and of the incident field, the total field will be independent of azimuth ϕ everywhere in circular cylindrical coordinate system (r, ϕ, z). Therefore, a scalar potential $\psi(r, z)$ which defines the acoustic pressure and velocity by $p = i\omega\rho_0\psi$ and $\mathbf{v} = \operatorname{grad}\psi$, respectively, is introduced. Here ρ_0 is the density of the undisturbed medium. Time dependence is assumed to be $e^{-i\omega t}$ and suppressed throughout this paper, where ω is the angular frequency. The incident sound wave which is propagating the positive z direction is taken to be

$$\psi_i(r, z) = A_0 J_0(\xi_n r/a) e^{i\zeta_n z}, \quad z \in \mathbb{R}, \tag{1a}$$

where ξ_n is the root of the equation

$$ikaJ_0(\xi_n)/Z_1 + \xi_n J_1(\xi_n) = 0, \tag{1b}$$

and ζ_n stands for

$$\zeta_n = \sqrt{k^2 - (\xi_n/a)^2}, \tag{1c}$$

$n = 1, 2, \ldots.$ Here $k = \omega/c$ denotes the wave number of the medium and c is the speed of sound. A_0 stands for the amplitude of the incident wave. An expression of the total field will be established as follows

$$\psi^{\mathrm{T}}(r, z) = \begin{cases} \psi_1(r, z), & r > a, \quad z \in (-\infty, \infty), \\ \psi_2(r, z), & r < a, \quad z > l_2, \\ \psi_3(r, z), & r < a, \quad 0 < z < l_2, \\ \psi_4(r, z), & r < a, \quad -l_1 < z < 0, \\ \psi_5(r, z) + \psi_i(r, z), & r < a, \quad z < -l_1, \end{cases} \tag{2}$$

$\psi_j(r,z),\ j = 1-5$, which satisfy the Helmholtz equation

$$\left[\frac{1}{r}\frac{\partial}{\partial r}\left(r\frac{\partial}{\partial r}\right)+\frac{\partial^2}{\partial z^2}+k^2\right]\psi_j(r,z) = 0, \quad j = 1-5 \tag{3}$$

are to be determined with the aid of the following boundary and continuity relations. The boundary condition on the absorbing surface can be given in terms of the potential funcitons ψ_3 and ψ_5

$$\left(ik/Z_1 - \frac{\partial}{\partial r}\right)\psi_5(a,z) = 0, \quad z < -l_1, \tag{4a}$$

$$\left(ik/Z_2 - \frac{\partial}{\partial r}\right)\psi_3(a,z) = 0, \quad 0 < z < l_2. \tag{4b}$$

The outer surface of the duct is rigid, so that

$$\frac{\partial}{\partial r}\psi_1(a,z) = 0, \quad z < l_2, \tag{4c}$$

and the inner duct wall is rigid for $-l_1 < z < 0$

$$\frac{\partial}{\partial r}\psi_4(a,z) = 0, \quad -l_1 < z < 0. \tag{4d}$$

Consider now the continuity conditions related to total field at $r = a$, $z > l_2$ which are given by

$$\frac{\partial}{\partial r}\psi_1(a,z) - \frac{\partial}{\partial r}\psi_2(a,z) = 0, \quad z > l_2, \tag{4e}$$

$$\psi_1(a,z) - \psi_2(a,z) = 0, \quad z > l_2. \tag{4f}$$

From the continuity at the point $z = l_2, 0, -l_1$, we get

$$\frac{\partial}{\partial z}\psi_2(r,l_2) - \frac{\partial}{\partial z}\psi_3(r,l_2) = 0, \quad r < a, \tag{4g}$$

$$\psi_2(r,l_2) - \psi_3(r,l_2) = 0, \quad r < a, \tag{4h}$$

$$\frac{\partial}{\partial z}\psi_3(r,0) - \frac{\partial}{\partial z}\psi_4(r,0) = 0, \quad r < a, \tag{4i}$$

$$\psi_3(r,0) - \psi_4(r,0) = 0, \quad r < a, \tag{4j}$$

$$\frac{\partial}{\partial z}\psi_4(r,-l_1) - \frac{\partial}{\partial z}\psi_5(r,-l_1) = \frac{\partial}{\partial z}\psi_i(r,-l_1), \quad r < a, \tag{4k}$$

$$\psi_4(r,-l_1) - \psi_5(r,-l_1) = \psi_i(r,-l_1), \quad r < a. \tag{4l}$$

Furthermore, to obtain a unique solution the following edge conditions at the mouth $r = a$, $z = l_2$ of the cylinder should be taken into account

$$\frac{\partial}{\partial r}\psi_1 = \mathbb{O}(z^{-1/2}), \quad z \to l_2. \tag{4m}$$

3. DERIVATION AND SOLUTION OF THE WIENER–HOPF EQUATION

The field $\psi_1(r,z)$, $r > a$ satisfy the Helmholtz equation for $z \in (-\infty,\infty)$. The following solution is obtained when (4c) is applied

$$F^-(r,\alpha) + F^+(r,\alpha) = -\dot{F}^+(a,\alpha)\frac{H_0^{(1)}(Kr)}{K(\alpha)H_1^{(1)}(Ka)}, \tag{5}$$

where $H_m^{(1)}$ is the Hankel function of the first type and $K(\alpha)$ is the square-root function $K(\alpha) = \sqrt{k^2 - \alpha^2}$ which is defined in the complex α-plane [14] and $F(r,\alpha)$ is the Fourier transform of the field $\psi_1(r,z)$ defined to be

$$F(r,\alpha) = \int_{-\infty}^{\infty} \psi_1(r,z) e^{i\alpha z} dz = e^{i\alpha l_2}[F^-(r,\alpha) + F^+(r,\alpha)], \tag{6}$$

where

$$F^-(r,\alpha) = \int_{-\infty}^{l_2} \psi_1(r,z) e^{i\alpha(z-l_2)} dz, \quad F^+(r,\alpha) = \int_{l_2}^{\infty} \psi_1(r,z) e^{i\alpha(z-l_2)} dz. \tag{7}$$

Owing to the analyticity of Fourier integrals, $F^+(r,\alpha)$ and $F^-(r,\alpha)$ are analytic functions of α in the upper and lower half α-planes defined by $\Im m\alpha > \Im m(-k)$ and $\Im m\alpha < \Im mk$, respectively. By applying the similar mathematical procedures in region $r < a$, $z > l_2$, the following equation is obtained [14]

$$G^+(r,\alpha) = \frac{1}{KJ_1(Ka)}\left[-\dot{F}^+(a,\alpha)J_0(Kr) + \int_0^a (f(t) - i\alpha g(t))Q(t,r,\alpha)tdt\right], \tag{8}$$

where

$$Q(r,t,\alpha) = \frac{\pi}{2}\begin{cases} J_0(Kr)[J_1(Ka)Y_0(Kt) - Y_1(Ka)J_0(Kt)], & r < t, \\ J_0(Kt)[J_1(Ka)Y_0(Kr) - Y_1(Ka)J_0(Kr)], & r > t. \end{cases} \tag{9}$$

Here, J_m and Y_m are the well-known Bessel and Neumann functions of order *m*. $G^+(r,\alpha)$ is an analytic function in the upper α-plane, defined by

$$G^+(r,\alpha) = \int_{l_2}^{\infty} \psi_2(r,z) e^{i\alpha(z-l_2)} dz, \tag{10}$$

while $f(r)$ and $g(r)$ stand for

$$f(r) = \sum_{m=0}^{\infty} f_m J_0(j_m r/a) = \frac{\partial}{\partial z}\psi_2(r,l_2), \tag{11a}$$

$$g(r) = \sum_{m=0}^{\infty} g_m J_0(j_m r/a) = \psi_2(r,l_2). \tag{11b}$$

The regularity of the right hand side of the equation (8) may be violated by the presence of the simple poles occurring at the zeros of $KJ_1(Ka)$ lying in the upper α-half plane, namely at $\alpha = \alpha_m$, satisfying

$$J_1(j_m) = 0, \quad m = 0,1,\ldots, \tag{12a}$$

$$\alpha_0 = k, \quad \alpha_m = \sqrt{k^2 - (j_m/a)^2}, \quad \Im m\alpha_m \geq \Im mk. \tag{12b}$$

These poles can be eliminated by imposing that their residues are zero. This gives

$$\dot{F}^+(a,\alpha_m) = \frac{a}{2} J_0(j_m)[f_m - i\alpha_m g_m]. \tag{13}$$

The evaluation of the integrals at the right-hand side of (8) after substituting (11a, b) yields

$$\frac{\dot{F}^+(a,\alpha)}{K^2(\alpha)M(\alpha)} - \frac{a}{2}F^-(a,\alpha) = \frac{a}{2}\sum_{m=0}^{\infty}\frac{J_0(j_m)}{\alpha_m^2 - \alpha^2}[f_m - i\alpha g_m] \tag{14}$$

which is the Wiener–Hopf equation valid in the strip $\Im m(-k) < \Im m\alpha < \Im mk$ [14]. Here

$$M(\alpha) = \pi i J_1(Ka) H_1^{(1)}(Ka). \tag{15}$$

The solution of (14) can easily be obtained through the classical Wiener–Hopf procedure,

$$\frac{\dot{F}^{+}(a,\alpha)}{(k+\alpha)M_{+}(\alpha)} = \frac{a}{2}\sum_{m=0}^{\infty}\frac{(k+\alpha_m)J_0(j_m)M_{+}(\alpha_m)}{2\alpha_m(\alpha+\alpha_m)}[f_m + i\alpha_m g_m]. \tag{16}$$

Here, $M_{+}(\alpha)$ and $M_{-}(\alpha)$ are analytic and free of zeros in the upper and lower half-planes, respectively. Wiener–Hopf factorization of the function $M(\alpha)$ as [14]

$$M(\alpha) = M_{+}(\alpha)M_{-}(\alpha), \quad M_{-}(\alpha) = M_{+}(-\alpha). \tag{17}$$

4. DETERMINATION OF THE COEFFICIENTS

In order to solve the problem by using the mode matching technique, the geometry is divided into three regions and the eigenfunction expansions and related orthogonality conditions in each waveguide region are determined. These regions are as follows:

$$R_1 : \{0 < z < l_2\}, \quad R_2 : \{-l_1 < z < 0\}, \quad R_3 : \{-\infty < z < -l_1\}. \tag{18}$$

4.1. Region 1 (R_1)

Eigenfunction expansion is applied in order to solve the given problem in various regions. The solution in this region can be written as

$$\psi_3(r,z) = \sum_{n=1}^{\infty}[A_n e^{i\varkappa_n z} + B_n e^{-i\varkappa_n z}]J_0(\tau_n r/a), \tag{19}$$

with

$$ikaJ_0(\tau_n)/Z_2 + \tau_n J_1(\tau_n) = 0, \quad n = 1,2,\ldots, \tag{20a}$$

$$\varkappa_n = \sqrt{k^2 - (\tau_n/a)^2}, \quad n = 1,2,\ldots . \tag{20b}$$

From the continuity relations which are given (4g, h), using (11a, b) and (19) one can write

$$\sum_{m=0}^{\infty} f_m J_0(j_m r/a) = i\sum_{n=1}^{\infty}\varkappa_n[A_n e^{i\varkappa_n l_2} - B_n e^{-i\varkappa_n l_2}]J_0(\tau_n r/a), \tag{21a}$$

$$\sum_{m=0}^{\infty} g_m J_0(j_m r/a) = \sum_{n=1}^{\infty}[A_n e^{i\varkappa_n l_2} + B_n e^{-i\varkappa_n l_2}]J_0(\tau_n r/a). \tag{21b}$$

Integrating over $[0,a]$ after multiplying the both sides of equation (21a) and (21b) with $J_0(\tau_n r/a)r$ which satisfy the orthogonality relation, we get

$$A_n = e^{-i\varkappa_n l_2}\frac{a^2\tau_n J_1(\tau_n)}{2i\varkappa_n P_n}\sum_{m=0}^{\infty}\frac{f_m + i\varkappa_n g_m}{\tau_n^2 - j_m^2}J_0(j_m), \tag{22a}$$

$$B_n = -e^{i\varkappa_n l_2}\frac{a^2\tau_n J_1(\tau_n)}{2i\varkappa_n P_n}\sum_{m=0}^{\infty}\frac{f_m - i\varkappa_n g_m}{\tau_n^2 - j_m^2}J_0(j_m), \tag{22b}$$

where

$$P_n = \frac{a^2}{2}[J_0^2(\tau_n) + J_1^2(\tau_n)]. \tag{23}$$

4.2. Region 2 (R_2)

In this region, $\psi_4(r,z)$ can be expressed as

$$\psi_4(r,z) = \sum_{n=0}^{\infty}[C_n e^{i\alpha_n z} + D_n e^{-i\alpha_n z}]J_0(j_n r/a), \tag{24}$$

where j_n and α_n are defined in (12a, b). Using the continuity relations at $z = 0$, we obtain

$$i\sum_{n=1}^{\infty}\varkappa_n[A_n - B_n]J_0(\tau_n r/a) = i\sum_{m=0}^{\infty}\alpha_m[C_m - D_m]J_0(j_n r/a), \tag{25a}$$

$$\sum_{n=1}^{\infty}[A_n + B_n]J_0(\tau_n r/a) = \sum_{m=0}^{\infty}[C_m + D_m]J_0(j_n r/a). \tag{25b}$$

A similar procedure is adopted to determine A_n and B_n which are obtained depending on the C_m and D_m

$$A_n = \frac{a^2\tau_n J_1(\tau_n)}{2\varkappa_n P_n}\sum_{m=0}^{\infty}\frac{J_0(j_m)}{\tau_n^2 - j_m^2}(\varkappa_n[C_m + D_m] + \alpha_m[C_m + D_m]), \tag{26a}$$

$$B_n = \frac{a^2\tau_n J_1(\tau_n)}{2\varkappa_n P_n}\sum_{m=0}^{\infty}\frac{J_0(j_m)}{\tau_n^2 - j_m^2}(\varkappa_n[C_m + D_m] - \alpha_m[C_m + D_m]). \tag{26b}$$

4.3. Region 3 (R_3)

For this region, the field can be written as

$$\psi_5(r,z) = \sum_{n=1}^{\infty}R_n e^{-i\zeta_n z}J_0(\xi_n r/a), \tag{27}$$

where R_n is the amplitude of the reflected duct mode in region 3. Here ξ_n and ζ_n are defined in (1b, c). From (4k, l), one writes

$$i\sum_{n=0}^{\infty}\alpha_n[C_n e^{-i\alpha_n l_1} - D_n e^{i\alpha_n l_1}]J_0(j_n r/a) = -i\sum_{m=1}^{\infty}\zeta_m R_m e^{i\zeta_m l_1}J_0(\xi_m r/a) + i\zeta_r e^{-i\zeta_r l_1}J_0(\xi_n r/a), \tag{28a}$$

$$\sum_{n=0}^{\infty}[C_n e^{-i\alpha_n l_1} + D_n e^{i\alpha_n l_1}]J_0(j_n r/a) = \sum_{m=1}^{\infty}R_m e^{i\zeta_m l_1}J_0(\xi_m r/a) + e^{-i\zeta_r l_1}J_0(\xi_n r/a). \tag{28b}$$

Similarly, C_n and D_n can be found easily

$$C_n = \frac{e^{i\alpha_n l_1}}{\alpha_n J_0(j_n)}\left[\sum_{m=1}^{\infty}R_m\frac{\xi_m J_1(\xi_m)}{\xi_m^2 - j_n^2}(\alpha_n - \zeta_m)e^{i\zeta_m l_1} + \frac{\xi_r J_1(\xi_r)}{\xi_r^2 - j_n^2}(\alpha_n + \zeta_r)e^{-i\zeta_r l_1}\right], \tag{29a}$$

$$D_n = \frac{e^{-i\alpha_n l_1}}{\alpha_n J_0(j_n)}\left[\sum_{m=1}^{\infty}R_m\frac{\xi_m J_1(\xi_m)}{\xi_m^2 - j_n^2}(\alpha_n + \zeta_m)e^{i\zeta_m l_1} + \frac{\xi_r J_1(\xi_r)}{\xi_r^2 - j_n^2}(\alpha_n - \zeta_r)e^{-i\zeta_r l_1}\right], \tag{29b}$$

consider (22a, b) together with (26a, b) and (29a, b), namely

$$\sum_{m=0}^{\infty}\frac{f_m + i\varkappa_n g_m}{\tau_n^2 - j_m^2}J_0(j_m) = \sum_{m=0}^{\infty}\sum_{s=1}^{\infty}E_{nms}^{+}R_s + \sum_{m=0}^{\infty}F_{nmr}^{+}, \tag{30}$$

$$\sum_{m=0}^{\infty}\frac{f_m - i\varkappa_n g_m}{\tau_n^2 - j_m^2}J_0(j_m) = -\sum_{m=0}^{\infty}\sum_{s=1}^{\infty}E_{nms}^{-}R_s - \sum_{m=0}^{\infty}F_{nmr}^{-}, \tag{31}$$

where

$$E_{nms}^{\pm} = \frac{J_0(j_m)}{\tau_n^2 - j_m^2}ie^{i\varkappa_n l_2}[\varkappa_n C_{ms}^1 \pm \alpha_m C_{ms}^2], \tag{32a}$$

$$F_{nmr}^{\pm} = \frac{J_0(j_m)}{\tau_n^2 - j_m^2}ie^{i\varkappa_n l_2}[\varkappa_n D_{mr}^1 \pm \alpha_m D_{mr}^2], \tag{32b}$$

$$C_{ms}^1 = \frac{2e^{i\zeta_s l_1}}{\alpha_m J_0(j_m)}\frac{\xi_s J_1(\xi_s)}{\xi_s^2 - j_m^2}[\alpha_m\cos(\alpha_m l_1) - i\zeta_s\sin(\alpha_m l_1)], \tag{33a}$$

$$C^2_{ms} = \frac{2e^{i\zeta_s l_1}}{\alpha_m J_0(j_m)} \frac{\xi_s J_1(\xi_s)}{\xi_s^2 - j_m^2}[i\alpha_m \sin(\alpha_m l_1) - \zeta_s \cos(\alpha_m l_1)], \tag{33b}$$

$$D^1_{mr} = \frac{2e^{-i\zeta_r l_1}}{\alpha_m J_0(j_m)} \frac{\xi_r J_1(\xi_r)}{\xi_r^2 - j_m^2}[\alpha_m \cos(\alpha_m l_1) + i\zeta_r \sin(\alpha_m l_1)], \tag{34a}$$

$$D^2_{mr} = \frac{2e^{-i\zeta_r l_1}}{\alpha_m J_0(j_m)} \frac{\xi_r J_1(\xi_r)}{\xi_r^2 - j_m^2}[i\alpha_m \sin(\alpha_m l_1) + \zeta_r \cos(\alpha_m l_1)]. \tag{34b}$$

By substituting $\alpha = \alpha_1, \alpha_2, \alpha_3, \ldots$ in (16) and using (13) one can obtain

$$\frac{J_0(j_r)[f_r - i\alpha_r g_r]}{(k+\alpha_r)M_+(\alpha_r)} = \sum_{m=0}^{\infty} \frac{(k+\alpha_m)J_0(j_m)M_+(\alpha_m)}{2\alpha_m(\alpha_r + \alpha_m)}[f_m + i\alpha_m g_m], \quad r = 0,1,\ldots. \tag{35}$$

Expressions given by (30), (31) and (35) are linear systems of algebraic equations which involve the unknown coefficients f_m, g_m and R_m. By solving this system numerically, the unknown coefficients can be determined.

5. FAR FIELD

The radiated field in the region $r > a$ can be obtained by taking the inverse Fourier transform of $F(r,\alpha)$. From (6) we write

$$\psi_1(r,z) = -\frac{1}{2\pi}\int_{\mathcal{L}} \frac{\dot{F}^+(a,\alpha)H_0^{(1)}(Kr)}{KH_1^{(1)}(Ka)} e^{-i\alpha(z-l_2)} d\alpha, \tag{36}$$

where $\mathcal{L}$ is a straight line parallel to the real α-axis, lying in the strip $\Im m(-k) < \Im m\alpha < \Im mk$. Utilizing the asymptotic expansion of $H_0^{(1)}(Kr)$ as $kr \to \infty$

$$H_0^{(1)}(Kr) = \sqrt{\frac{2}{\pi Kr}} e^{iKr - i\pi/4}. \tag{37}$$

In (36), the integral can be evaluated through the saddle-point formula [21], we have

$$\psi_1(R,\theta) \sim D(\theta)\frac{e^{ikR}}{kR}, \tag{38}$$

where $D(\theta)$ is directivity given by

$$D(\theta) = \frac{ika}{2\pi} \frac{M_+(-k\cos\theta)(1-\cos\theta)}{\sin\theta H_1^{(1)}(ka\sin\theta)} \sum_{m=0}^{\infty} \frac{(k+\alpha_m)J_0(j_m)M_+(\alpha_m)}{2\alpha_m(\alpha_m - k\cos\theta)}[f_m + i\alpha_m g_m]. \tag{39}$$

Here, R and θ are the usual spherical coordinates, defined by

$$r = R\sin\theta, \quad z - l_2 = R\cos\theta. \tag{40}$$

6. NUMERICAL RESULTS

In this section, sound pressure level (SPL) is calculated numerically for the similar problem parameters as in the study of [15]. The following expression is used to give graphical plots for the sound pressure level

$$SPL = 20\log_{10}\left|\frac{p}{2\times 10^{-5}}\right|,$$

where p is the amplitude of the acoustic pressure of the sound wave, with the observation angle θ changing from 0 to π. The far field values are plotted at a distance 46 m away from the pipe edge [22]. The geometry parameters which remain unchanged in all examples, are given in Table 1.

Table 1. Parameter values for figures

Truncation number	(N)	10
Density of Un. Med.	(ρ_0)	1.255 kg/m^3
Speed of sound	(c)	340.17 m/s
Far radius	(r)	46 m
Duct radius	(a)	0.10 m
Duct extension	(l_2)	0.10 m

All the numerical results are derived by truncation of the infinite series and the infinite systems of linear algebraic equations after the first N terms. It is seen that the amplitude of the sound pressure level becomes insensitive to the increase at the truncation number after $N = 10$. Figure 2 shows the variation of the sound pressure level versus observation angle θ for different values of Z_1 with $l_1 = 0.1$ m, $f = 4000$ Hz and $Z_2 = 1 - 3i$. It is observed that the sound pressure level decreases with lining Z_1 ($z < -l_1$) compared to the rigid case ($Z_1 \to \infty$), as expected. In Fig. 3, the sound pressure level also decreases with lining Z_2 (duct extension) like in Fig. 2.

Figure 4 shows the variation of the amplitude of the sound pressure level against the observation angle for rigid-lined cases. It is observed that the sound pressure level decreases with absorbing lining compared to the fully rigid case. Notice that an oscillatory behavior is related to increasing value of frequency. An extra real root of α_m occurs when the frequency increases. A similar oscillatory effect can be seen with increasing value of duct radii like the frequency.

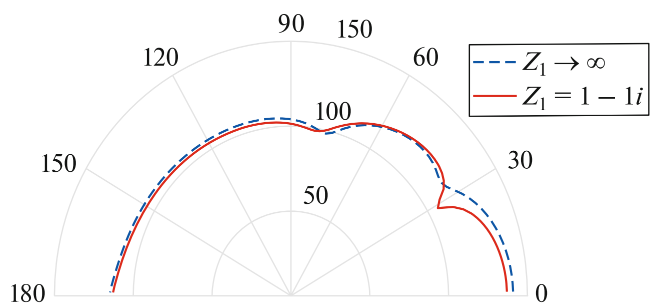

Fig. 2. Sound pressure level versus the observation angle for different values of Z_1 with $l_1 = 0.10$ m, $f = 4000$ Hz and $Z_2 = 1 - 3i$.

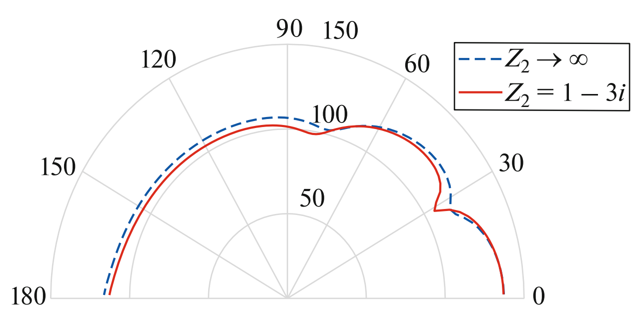

Fig. 3. Sound pressure level versus the observation angle for different values of Z_2 with $l_1 = 0.10$ m, $f = 4000$ Hz and $Z_1 = 1 - 1i$.

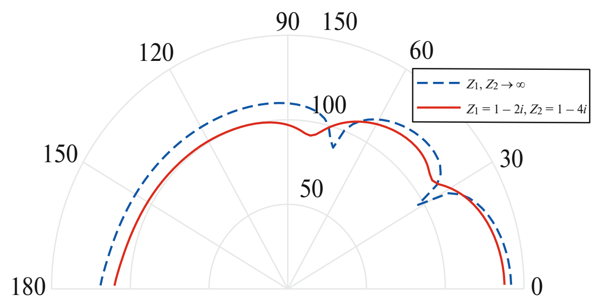

Fig. 4. Sound pressure level versus the observation angle for fully hard-lined pipe with $l_1 = 0$ and $f = 4000$ Hz.

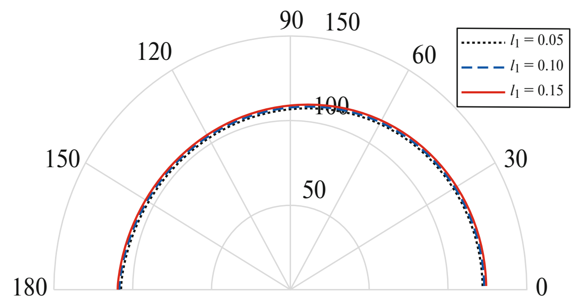

Fig. 5. Sound pressure level versus the observation angle for different values of l_1 with $f = 1500$ Hz, $Z_1 = 1 - 1i$ and $Z_2 = 1 - 3i$.

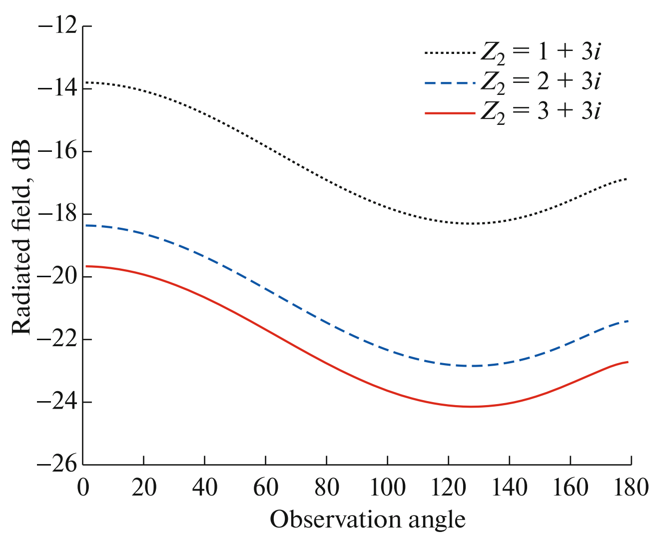

Fig. 6. Comparison of the sound pressure level versus the observation angle with the study of [14] for $Z_1 \to \infty$, $ka = 1$, $kl_1 = 0$ and $kl_2 = 10$.

Figure 5 depicts the variation of the sound pressure level against the observation angle θ for different values of l_1 with $f = 1500$ Hz, $Z_1 = 1 - 1i$ and $Z_2 = 1 - 3i$. The effect of the length of the inner rigid part provided a few decibel of sound wave variation. It is seen that the sound pressure level increases slightly as the l_1 is moved further into the duct.

Figure 6 depicts an excellent agreement for radiated field between the present paper and the previous study [14]. When the first interior lining (Z_1) is absent, i.e., $Z_1 \to \infty$, Fig. 6 is obtained. Notice that the curves corresponding to $Z_1 \to \infty$ coincide exactly with the results obtained in the previous paper by the authors [14, Fig. 5b]. This comparison is also important for the accuracy of the mathematical results. Note that $20\log_{10}|D(\theta)|$ is used to make comparison for Fig. 6.

7. CONCLUSION

Radiation of sound waves comprising of semi-infinite duct with different inner lining is presented. The part of the inner surface of the duct is assumed to be rigid. Wiener–Hopf technique has been engaged to obtain sound pressure level. Here, inner partial rigidity makes the problem more complicated. The problem first reduced Wiener–Hopf equation and solved by using the classical factorization and decomposition procedures. The solution involves three systems of linear algebraic equations involving three sets of infinitely many unknown expansion coefficient. Numerical results are obtained graphically for various values of the problem parameters. At certain angles, it has been observed that the sound pressure level for the relatively high frequency is less sensitive to the variations of the length of the inner rigid piece.

In the case where the effect of the Z_1 is absent ($Z_1 \to \infty$), the results obtained in this paper are compared with the results of [14] and the results are found to be in good agreement.

CONFLICT OF INTEREST

The authors declare that they have no conflicts of interest.

REFERENCES

1. R. Munt, "The interaction of sound with a subsonic jet issuing from a semi-infinite cylinder," J. Fluid Mech. **83**, 609–640 (1977).
2. I. D. Abrahams, "Scattering of sound by two parallel semi-infinite screens," Wave Motion **9**, 289–300 (1987).
3. A. Büyükaksoy and A. Demir, "Diffraction of sound waves by a rigid cylindrical cavity of finite length with an internal impedance surface," Z. Angew. Math. Phys. **56**, 694–717 (2005).
4. G. Gabard and R. J. Astley, "Theoretical model for sound radiation from annular jet pipes: Far- and near-field solutions," J. Fluid Mech. **549**, 315–341 (2006).
5. B. Veitch and N. Peake, "Acoustic propagation and scattering in the exhaust flow from coaxial cylinders," J. Fluid Mech. **613**, 275–307 (2008).
6. A. Demir, "Scattering matrices in non-uniformly lined ducts," Z. Angew. Math. Phys. **68**, Article 8 (2017). https://doi.org/10.1007/s00033-016-0754-8
7. H. Levine and J. Schwinger, "On the radiation of sound from an unflanged circular pipe," Phys. Rev. **73**, 383–406 (1948).
8. B. Noble, *Methods Based on the Wiener–Hopf Techniques for the Solution of Partial Differential Equations* (Pergamon, London, 1958).
9. A. Büyükaksoy and B. Polat, "Diffraction of acoustic waves by a semi-infinite cylindrical impedance pipe of certain wall thickness," J. Eng. Math. **33** (4), 333–352 (1998).
10. G. Çınar, H. Öztürk, and Ö. Y. Çınar, "Reflection and transmission of plane acoustic waves in an infinite annular duct with a finite gap on the inner wall," Math. Methods Appl. Sci. **34**, 220–230 (2011).
11. A. Snakowska, J. Jurkiewicz, and L. Gorazd, "A hybrid method for determination of the acoustic impedance of an unflanged cylindrical duct for multimode wave," J. Sound Vib. **396**, 325–339 (2017).
12. B. Tiryakioglu, "Radiation of sound by a coaxial waveguide with semi-infinite perforated duct," Waves Random Complex Media (2020). https://doi.org/10.1080/17455030.2020.1782511
13. A. D. Rawlins, "Radiation of sound from an unflanged rigid cylindrical duct with an acoustically absorbing internal surface," Proc. R. Soc. A **361**, 65–91 (1978).
14. A. Demir and A. Buyukaksoy, "Radiation of plane sound waves by a rigid circular cylindrical pipe with a partial internal impedance loading," Acta Acust. Acust. **89**, 578–585 (2003).
15. B. Tiryakioglu, "Sound radiation from the perforated end of a lined duct," Acta Acust. Acust. **105** (5), 591–599 (2019).

16. B. Tiryakioglu, "Radiation of acoustic waves by a partially lined pipe with an interior perforated screen," J. Eng. Math. **122** (1), 17–29 (2020).

17. B. Nilsson and O. Brander, "the propagation of sound in cylindrical ducts with mean flow and bulk-reacting lining: I. Modes in an infinite duct," J. Inst. Math. Appl. **26** (3), 269–298 (1980).

18. M. Hassan and A. D. Rawlins, "Sound radiation in a planar trifurcated lined duct," Wave Motion **29**, 157–174 (1999).

19. S. W. Rienstra, "Acoustic scattering at a hard-soft lining transition in a flow duct," J. Eng. Math. **59**, 451–475 (2007).

20. N. Peake and I. D. Abrahams, "Sound radiation from a semi-infinite lined duct," Wave Motion **92**, 102407 (2020).

21. R. Mittra and S. W. Lee, *Analytical Techniques in the Theory of Guided Waves* (Macmillan, New York, 1971).

22. A. Demir and S. W. Rienstra, "Sound radiation from a lined exhaust duct with lined afterbody," in *16th AIAA/CEAS Aeroacoustics Conference, AIAA Paper 2010-3947* (Stockholm, Sweden, 2010).